Phase-specific stable isotope fractionation effects during combined gas-liquid phase exchange and biodegradation

Ali M. Khan[1], Mehdi Gharasoo[2], Lukas Y. Wick[1], Martin Thullner[1,*]

[1] *Department of Environmental Microbiology, UFZ - Helmholtz Centre for Environmental Research, Leipzig, Germany*

[2] *Department of Earth and Environmental Sciences, University of Waterloo, Waterloo, Ontario, Canada*

[*] Corresponding author: Mailing address: Federal Institute for Geosciences and Natural Resources (BGR); Stilleweg 2; 30655 Hannover, Germany. phone: +49 511 643 3077, e-mail: martin.thullner@bgr.de.

ABSTRACT

Stable isotope fractionation of toluene under dynamic phase exchange was studied aiming at ascertaining the effects of gas-liquid partitioning and biodegradation of toluene stable isotope composition in liquid-air phase exchange reactors (Laper). The liquid phase consisted of a mixture of aqueous minimal media, a known amount of a mixture of deuterated (toluene-d) and non-deuterated toluene (toluene-h), and bacteria of toluene degrading strain *Pseudomonas putida* KT2442. During biodegradation experiments, the liquid and air-phase concentrations of both toluene isotopologues were monitored to determine the observable stable isotope fractionation in each phase. The results show a strong fractionation in both phases with apparent enrichment factors beyond -800‰. An offset was observed between enrichment factors in the liquid and the gas phase with gas-phase values showing a stronger fractionation in the gas than in the liquid phase. Numerical simulation and parameter fitting routine was used to challenge hypotheses to

explain the unexpected experimental data. The numerical results showed that either a very strong, yet unlikely, fractionation of the phase exchange process or a – so far unreported – direct consumption of gas phase compounds by aqueous phase microorganisms could explain the observed fractionation effects. The observed effect can be of relevance for the analysis of volatile contaminant biodegradation using stable isotope analysis in unsaturated subsurface compartments or other environmental compartment containing a gas and an liquid phase.

Keywords: VOC, toluene phase exchange, stable isotope fractionation, bioavailability, biodegradation, CSIA.

INTRODUCTION

Volatile organic compounds (VOCs) such as BTEX (i.e., benzene, toluene, ethylbenzene, and xylene) are frequently found contaminants in soils and aquatic environments and continue to be the major source of air pollution. These aromatic hydrocarbons are of particular concern due to their relatively high water solubility, toxicity and environmental mobility (Rolle and Jin, 2017; Wiedemeier et al., 1999). Compound specific isotope analysis (CSIA) is a powerful tool to trace the fate of organic contaminants in the environment. It is based on the shift in isotope composition of the target compounds due to chemical reactions or biodegradation (Blum et al., 2009; Elsner, 2010; Elsner et al., 2012; Kopinke et al., 2018; Thullner et al., 2012). To understand and quantify contaminant transport and (bio-)transformation mechanisms, labelled and non-labelled organic compound mixtures have often been applied as a diagnostic tool (Horst et al., 2016). In two-phase (air-water) systems, many VOCs show inverse isotope effects for elements such as hydrogen and carbon, which means that the liquid phase becomes more depleted in the heavier isotopes during volatilization; approaches to explain these inverse effects were presented by Baertschi and Kuhn (1957), Bigeleisen (1961), Wolfsberg (1963) and Horst et al. (2016): usually, the obtained fractionation data are explained and

quantitatively interpreted in terms of the established two-film theory (Schwarzenbach et al., 2003) resulting in diffusion-controlled and equilibrium-controlled fractionation coefficients (Kopinke et al., 2018).

Although many studies reported on vapor pressure isotope effects of pure organic compounds (Horst et al., 2016), only few described isotope effects for organics dissolved in water and under equilibrium conditions (Horst et al., 2016; Hunkeler and Aravena, 2000; Slater et al., 1999). However, in the environment, organic compounds such as toluene are often water-dissolved and phase transfer may occur under non-equilibrium or kinetic conditions (Horst et al., 2016). Observed fractionation effects thereby were found to be different for the 'forward' and the 'reverse' partitioning, i.e. from the aqueous into an organic solvent phase and *vice versa* (Kopinke et al., 2018).

Motivated by this shortage of available data and lack of basic understanding, we measured relative phase exchange between gas phase and aqueous phase of isotopologues (non-labelled and fully deuterated) of toluene by means of a two-phase partitioning approach under dynamic conditions that were driven by the biodegradation of toluene in the aqueous phase. To our knowledge, no study has reported a comparison of stable isotope fractionation in the aqueous phase and the gas phase simultaneously.

Hence, we here report and discuss the unexpected fractionation behavior of toluene in the gas phase and liquid phase. We present isotope effects associated with non-equilibrium volatilization of toluene dissolved in water in liquid-air phase exchange reactors (Laper) and test hypotheses for the effects observed using a numerical modeling approach.

MATERIALS & METHODS

Liquid-Air Phase Exchange Reactors (Laper)

Gastight chromoflax glass bottles with a total volume of 1150 mL (**series A**) and 2375 mL (**series B**) were used as Laper. Each of these neck bottles had a main opening at the top and sampling ports on the top right and bottom left side (**Fig. 1**). Laper reactors contained magnetic stirrer bars (25 x 6 mm) and were kept on magnetic shakers (250 rpm). The reactors were filled with liquid minimal medium, i.e., 200 mL in series A and

400 mL in series B. One abiotic "control" and duplicate bioreactive Laper (cf. Laper 1 and Laper 2) were run in parallel in each series at 22-23 °C. Series A also includes a third experimental run (Laper 3) operated under the above-mentioned conditions at an earlier date. The remaining volumes of 950 mL and 1975 mL in series A and series B, respectively, were categorized as headspace. Reactors were operated under closed conditions and had sufficient amount of oxygen in the headspace for complete aerobic biodegradation of the known amounts of VOCs toluene-h and toluene-d (20 µL pure phase of a 1:1 mixture of toluene-h and toluene-d for series A and 40 µL for series B). The VOCs were spiked to the liquid media and then the media were stirred by the help of a magnetic stirrer bar. The Lapers were kept on magnetic shakers for 12 hours to equilibrate prior to the start of the sampling. Calculated equilibrium concentrations of total toluene (toluene-h and toluene-d) were between 9 and 11 mg L^{-1} in the gas phase and between 32 and 45.8 mg L^{-1} in the liquid phase (assuming a Henry volatility constant between 0.2 and 0.35 (Sander, 2015)). Additionally, methyl tert-butyl ether (MTBE) (20 µL pure phase) was added as tracer. MTBE was found to be non-reactive, i.e., non-biodegradable at given conditions. Note that the resulting liquid concentrations were far below the maximum solubility of the compounds which ensures are complete dissolution of the pure phase spiked to the liquid media.

Pseudomonas putida KT2442 DsRed pWW0 gfp (Nancharaiah et al., 2003), was cultured following the protocol mentioned in Kampara et al. (2008) and Khan et al. (2016). The cells were added to the Laper just before the start of the experiments with OD_{578nm} = 0.1 (equivalent to ≈2 × 10^7 cfu mL^{-1}) in the reactors at the start of the experiments. Laper allowed for gas-tight sampling of liquid and gas-phase VOCs (Supplementary Material, **Fig. 1**). First samples were taken immediately after the addition of bacteria denoted as t0 (0 hours). Subsequent samples were taken hourly until t8 (8 hours). Gas-phase and liquid samples (500 µL each) were analyzed by headspace GC as detailed in Khan et al. (2016). These closed systems can suitably be analyzed by the Rayleigh model approach. An observation period between t0 and t8 was selected for the isotope analysis and data were

analyzed by plotting the logarithmic form of the Rayleigh equation for deuterated compounds (Hunkeler, 2002) to determine stable isotope enrichment factors.

Tested hypotheses using a numerical routine

Two hypotheses on possible processes taking place in the batch systems were tested for explaining the observed changes stable hydrogen isotope signatures of toluene: *Hypothesis 1* assumes an exchange of toluene between the liquid and gas phase in addition to the microbial toluene degradation in the liquid phase. Both processes were considered to cause a stable hydrogen isotope fractionation of toluene and a computational reaction scheme was set up for their description. For this, the two isotopologues were considered as independent reactive species with concentrations: ${}^{l}c_d$, ${}^{h}c_d$, ${}^{l}c_g$ and ${}^{h}c_g$; the indices *h* and *l* are indicating the heavy (deuterated) and light (non-deuterated) isotopologue, and the indices *g* and *d* are indicating the gas phase and the liquid (dissolved) phase. The phase exchange between the liquid and the gas phase was described by a linear exchange term and the microbial degradation in the liquid phase by Michaelis-Menten kinetics in an isotope-specific version (Khan et al., 2018; Thullner et al., 2008). This results in a set of rate expressions:

$$ {}^{l,h}r_1 = {}^{l,h}k_{ex} \cdot \left({}^{l,h}c_g - {}^{l,h}c_d \cdot {}^{l,h}H \right) \quad \text{(phase exchange liquid-gas)} \quad \text{(eq. 1)} $$

$$ {}^{l}r_2 = k_{max} \cdot \frac{{}^{l}c_d}{K_s + {}^{l}c_d + {}^{h}c_d \cdot \alpha_b} \quad \text{(degradation of toluene-h)} \quad \text{(eq.2)} $$

$$ {}^{h}r_2 = k_{max} \cdot \alpha_b \cdot \frac{{}^{h}c_d}{K_s + {}^{l}c_d + {}^{h}c_d \cdot \alpha_b} \quad \text{(degradation of toluene-d)} \quad \text{(eq. 3)} $$

${}^{h,l}H$ is the dimensionless Henry volatility, k_{max} is the maximum degradation rate, K_s is the Michaelis-Menten constant and α_b the stable isotope fractionation factor of the degradation reaction. The rate parameters ${}^{l,h}k_{ex}$ of the phase exchange are linked via the stable isotope fractionation factor α_{ex} of the phase exchange (${}^{h}k_{ex} = \alpha_{ex} \cdot {}^{l}k_{ex}$). Note that fractionation factors and the associated enrichment factors are linked via $\varepsilon_{b,ex}[‰] = (\alpha_{b,ex} - 1)/1000$.

Hypothesis 2 considers in addition to the processes described in *Hypothesis 1* another biodegradation processes which acts directly on the gas phase concentration. This is

motivated by the observation that microorganisms located directly at the liquid-gas interface can have direct access to the vapor phase substrate (Hanzel et al., 2011). Analogous to the liquid-phase degradation an isotope-specific version of Michaelis-Menten kinetics is used to describe this additional process:

$$ {}^{l}r_3 = k_{max,g} \cdot \frac{{}^{l}c_g}{K_s / {}_{l}H + {}^{l}c_g + {}^{h}c_g \cdot \alpha_{b,g}} $$

(gas-phase degradation of toluene-h) (eq. 4)

$$ {}^{h}r_3 = k_{max,g} \cdot \alpha_{b,g} \cdot \frac{{}^{h}c_g}{K_s / {}_{h}H + {}^{l}c_g + {}^{h}c_g \cdot \alpha_{b,g}} $$

(gas-phase degradation toluene-d) (eq. 5)

with $k_{max,g}$ as the maximum degradation rate and $\alpha_{b,g}$ ($\varepsilon_{b,ex}[‰] = (\alpha_{b,g} - 1)/1000$) as the stable isotope fractionation factor of this additional degradation reaction.

The two different schemes were implemented into the numerical modeling and fitting framework ReKinSim (Gharasoo et al., 2017) which allows to determine parameter values best suited to describe the measured data even for such a kinetically complex reaction system. For each reactive Laper system best-fit parameters were determined using different constraints on their values.

RESULTS AND DISCUSSION

Measured toluene stable isotope fractionation in Laper

Initial liquid and gas-phase concentrations of total toluene ranged from ca. 30 -50 mg $L^{-1}$and 10.5 to 11 mg L^{-1}, resp. While there were experimental variations in the liquid concentrations, the gas phase concentrations exhibited only very minor experimental errors. See Supplementary Material, **Figs. S1 and S2** for a complete overview of all measured concentrations.

Toluene concentrations from the abiotic control experiments and MTBE-tracer concentrations showed no major changes during the experiment and indicate that there were no underlying processes beside biodegradation that may have led to toluene removal

(Supplementary Material, **Figs. S1 and S2**). Stable isotope enrichment factors in the controls of ε_v = -5 to -29‰ in the vapor phase and ε_l = 0 to -2‰ in the liquid phase very small (**Fig. 2A and 2E**) and further confirmed the absence of microbial activity that would account for ε of up to -920‰ (Khan et al., 2018). Such low values may be attributed to the combined physical processes such as sorption (Fischer et al., 2006), isotopic mass differences, but might just also reflect the noise level of the measurements.

In contrast to the control experiments, toluene concentrations declined by approximately 50% within 8 h in all bioreactive Lapers (cf. Lapers 1-3) due to biodegradation. In Laper 3 changes of the bacterial optical density (OD_{578nm}) was further measured showing an increase from 0.1 to 0.22 within 8 hours as observed previously (Kampara et al., 2009; Kampara et al., 2008). The associated hydrogen isotope enrichment factors in the Lapers varied between ε = -810‰ and -837‰ for the liquid phase (with one outlier of -706‰), and ε = -873‰ and -923‰ for the gas phase (**Fig. 2**) confirming biodegradation as predominant removal process. Observed gas phase enrichment factors hence are in good agreement with earlier reports (ε = -920‰ ± 50‰, Khan et al. (2018)) and with studies on toluene degradation in liquid batch systems by a similar strain (ε = -905‰ ± 71‰, Morasch et al. (2001); ε = -934‰ ± 21‰, Kampara et al. (2008)). However, less fractionation in the liquid than in the gas phase was observed in all Lapers leading to an offset of 91‰ ± 50‰ between ε values of the two phases. With this standard deviation the confidence for the fractionation in the gas phase being stronger that in the liquid phase is larger than 95% which indicates significance (Ross, 2017). Following Scott et al. (2004) regression lines were not forced through the origin, however forcing the regression lines through the origin would have led to even larger differences between the enrichment factors observed in the two phases.

Given that degradation is likely to take place in the liquid phase only, the weaker fractionation in the liquid phase hence can not be explained by masking effects due to mass transfer limitations (Thullner et al., 2013) that would have led to less fractionation in the gas phase than in the liquid phase. Results for series A and series B obtained for

198 similar yet different experimental systems were highly comparable which indicates that
199 the observed effects are not linked to any specific reactor setup.
200
201 ***Hypothesis testing***
202 Numerical results for *Hypothesis 1* (i.e. toluene degradation in the liquid phase and a
203 phase exchange between liquid and gas phase contribute to stable hydrogen isotope
204 signatures; cf. eqs. 1-3) allowed for an adequate fitting of the observed concentrations in
205 the liquid and the vapor phase for both, series A and the series B systems (Supplementary
206 Material, **Figs. S3 and S4**). Also the magnitude of the observed fractionation effects and,
207 in particular, the stronger fractionation in the gas than in the liquid phase could be fitted
208 well (**Fig. 3**). The obtained values of the fitting parameters are comparable to previous
209 studies yet show some variability between the different batch systems (cf. **Table 1** for all
210 obtained fitting parameters values). For a detailed sensitivity analysis of model results
211 using a similar set equations see e.g., Gharasoo et al. (2019).
212 For matching the observed gap between the isotope enrichment factors in the liquid and
213 the vapor phase, however, extremely high kinetic enrichment factor for the phase
214 exchange process (ε_{ex}) of $\varepsilon_{ex} \approx$ -900‰ to -500‰ (**Table 1**) had to be inserted.
215 Constraining ε_{ex} to an arbitrary range of -100‰ to 0‰ (i.e., a significant yet probably
216 more reasonable fractionation due to the phase exchange) did not allow to reproduce the
217 observed stronger fractionation in the vapor phase as compared to the liquid phase
218 (Supplementary Material, **Figs. S3 and S4**). For the above described results no
219 equilibrium fractionation effect for the phase exchange was considered (i.e. $^{h}H = {}^{l}H$ with
220 no difference in gas phase and liquid phase isotope signatures at steady state) as the
221 abiotic control experiments showed no such fractionation effects. However, allowing ^{h}H
222 to differ from ^{l}H in the numerical simulations did not improve the fitting results. Also
223 including microbial growth into the reaction scheme (cf. doubling of biomass in Laper 3)
224 would not improve the ability to reproduce the gap between vapor phase and liquid phase
225 fractionation effects without considering the very high fractionation associated with the
226 phase exchange.

227 Fitting results suggest that the only remaining technical explanation of the observed
228 fractionation effects would be a very strong kinetic fractionation by the phase exchange
229 between the vapor and the liquid phase. To the best of our knowledge however, no
230 hydrogen fractionation data for deuterated toluene for water-air partitioning exist, and we
231 are not aware of such low phase exchange enrichment factors (i.e., high negative value)
232 for other compounds. For instance, Bouchard et al. (2018) report for the later hydrogen
233 enrichment factor a value of -5‰ for toluene with a single deuterium atom and Kuder et
234 al. (2009) report for values in the order of -10‰ for aromatic compounds with a single
235 deuterium atom. Scaling the later value linearly with the number of deuterated atoms
236 would lead to values in the order of -100‰ for fully deuterated compounds, which did
237 not allow reproducing the measured data and is still much lower than the phase-exchange
238 enrichment factors values needed to fit the measured data. The low phase exchange
239 enrichment factors needed to fit the data would imply a difference in molecular mobility
240 of approximately one order of magnitude. The fact that the mass difference between
241 toluene-h and toluene-d is approximately 8% and published differences between the
242 aqueous molecular diffusion coefficients of toluene-h and toluene-d do not exceed 0.38%
243 (Sun et al., 2021b) further implies against such differences in mobility. However, the low
244 fitted values of gas-liquid phase exchange fractionation factors might be due to the
245 increasing presence of the microorganisms which has been shown to increase the
246 contaminant mass-transfer coefficient by factor of 10 to 15 compared to the abiotic
247 conditions (Aeppli et al., 2009; Marozava et al., 2019). The fitted rate parameters for the
248 gas-liquid phase exchange are one order of magnitude higher than values estimated by
249 Khan et al. (2018) for similar systems assuming a diffusive boundary layer. Whether such
250 accelerated phase exchange has been taken place in the investigated batch systems can
251 not be verified based on the measured data. Furthermore, it remains to be clarified if
252 microbially induced acceleration would really enable the extreme phase-exchange
253 enrichment factor needed to explain the observed fractionation effects.
254 Accumulating microorganisms at the liquid-gas interface are also considered in
255 *Hypothesis 2*, which additionally considers them to take up and degrade toluene directly

256 from the gas phase. Such assumption leads to two independent degradation processes (one
257 acting on the liquid-phase concentration, one acting on the gas-phase concentration); each
258 with its own fractionation factor. When assuming the absence of any phase exchange
259 processes both phases would be decoupled and act as independent system and the
260 experimentally determined fractionation factors can be directly assigned to the
261 degradation process for each phase. However, for the liquid phase, this would require
262 enrichment factors ε between -840‰ and -710‰ which clearly differs from the value of
263 -920‰ ± 50‰ determined by Khan et al. (2018). Furthermore, there would be no
264 justification for neglecting a phase exchange in the system. Fitting the entire set of
265 reactions for *Hypothesis 2* (phase exchange, biodegradation acting on liquid-phase
266 concentration and biodegradation acting on gas-phase concentration; cf. eqs. 1-5) to the
267 measured data (cf. **Table 2** for an overview of all fitting parameters) allowed for an
268 adequate reproduction of measured concentrations (Supplementary Material, **Fig. S5 and**
269 **S6**). Also the fractionation effects for the series B systems could be fitted without
270 imposing any constraints on the value of the phase exchange rate parameter (**Fig. 4G to**
271 **4J**). To obtain a stronger fractionation in the gas than in the liquid phase in the series A
272 systems (**Fig. 4A to 4F**), it was however necessary to limit the value of the phase
273 exchange parameter to values similar to the best fit values for the series B systems. With
274 this additional constraint the experimentally determined effect could be reproduced for
275 two of the three series A systems. The range of the fitted/constrained values for the phase
276 exchange rate parameter are now similar to the values presented by Khan et al. (2018)
277 indicating that the magnitude of the phase exchange can be explained by a diffusive
278 boundary layer at the liquid-gas interface. The enrichment factor assigned to this phase
279 exchange was constrained approximately by range of reported aqueous molecular
280 diffusion induced fractionation (Sun et al., 2021b). While for some systems this fitted
281 valued of the phase-exchange enrichment factors suggest this process to contribute to the
282 fractionation observed in the system, best fits for other systems do not suggest this
283 fractionation effect to take place (i.e. $\varepsilon_{ex} = 0$‰).
284

Dynamic phase exchange implications

Our reactors showed that the phase exchange between liquid phase and gas phase has an unexpected, strong influence on the observed stable isotope fractionation. So far, only the masking of isotope signatures due to phase exchanges have been reported for two-phase systems, where a compound get degraded in the liquid phase after transfer from an organic phase (Aeppli et al., 2009; Marozava et al., 2019). Such systems behave analogously to single phase systems where the substrate concentrations are so low that mass-transfer to the cell or across the cell membrane acts as an effective rate-limiting step (Ehrl et al., 2018; Ehrl et al., 2019; Gharasoo et al., 2019; Kampara et al., 2009; Kampara et al., 2008; Sun et al., 2021a). Our results consistently show stronger fractionation (i.e. less negative hydrogen isotope enrichment factors) in the gas phase with differences being in the order of 50-100‰ and being independent of the concentrations measured. This trend is opposite to expectations for liquid phase biodegradation and phase-exchange between gas phase and liquid phase as rate limiting step masking toluene fractionation in the gas phase.

Equilibrium fractionation effects may also be excluded as the control experiments and the fitting results did not show any indications for this. Observed effects could rather be explained by the phase transition itself causing a fractionation. While such effects have been observed before (Jeannottat and Hunkeler, 2012; 2013), they would have to be extremely strong to explain the high differences of ε observed in the gas- and liquid phase given the fast (i.e. not strongly rate limiting) phase exchange. For non-deuterated toluene hydrogen enrichment factors values of -5‰ reported for the liquid-gas phase exchange have a similar magnitude than values of -2‰ to -10‰ reported for aerobic biodegradation of non-deuterated toluene (Bouchard et al., 2018). The results of this study would suggest that also for deuterated toluene enrichment factor values for the liquid-gas phase exchange are similar to enrichment factor values for aerobic biodegradation, but it must be doubted if such strong phase-exchange fractionation is indeed the case. This suggests that additional processes not known at this stage may have influenced the stable isotope fractionation observed in the experiments. We tested one of these assumptions (i.e. direct uptake of volatile compounds from the gas phase by aqueous phase microorganisms at

the gas-liquid interface) and showed that this additional process would explain the observed fractionation phenomena. A direct uptake has not been shown so far and thus any mechanistic explanation would be highly speculative. However, it has been shown that microorganisms can respond to gas phase concentration gradients (Hanzel et al., 2010; Hanzel et al., 2011).

Regardless of their eventual explanation, the observed effects appeared consistently and reproducibly in a series of experiments with each single experiment showing the discussed effects – although not at a significant level. However, the observed effects are statistically significant considering the entire set of five Laper systems. This indicates that our observations are not a simple statistical variation but represent an existing phenomenon.

Environmental implication

In the recent years, stable isotope fractionation effects associated with the aqueous-gas phase transition of volatile contaminants received a growing interest (Horst and Lacrampe-Couloume, 2020; Horst et al., 2016; Rostkowski et al., 2021), as phase-transfer processes are considered to be of potential relevance for the fate of VOCs in the gas phase (Bouchard et al., 2008; Khan et al., 2018)) as well as in the aqueous phase of subsurface environments (Horst and Lacrampe-Couloume, 2020). Up to know, the magnitude of such phase-transition related fractionation effects are either linked to differences in the diffusion coefficients of the different isotopologues (Kopinke et al., 2018), to molecular interactions in the aqueous phase (Julien et al., 2017; Rostkowski et al., 2021) or considered to mask fractionation effects of the contaminant degradation (Aeppli et al., 2009; Thullner et al., 2013). Our results show that additional stable isotope fractionation effects – not expected from the above processes – may have to be considered when using CSIA for assessing the fate of volatile contaminants in the subsurface compartments allowing for an aqueous-gas phase transition of the contaminants. Furthermore, the occurrence and magnitude of these additional processes might be triggered by the contaminant degradation process, which challenges their prediction in complex

biodegradation settings based on the isolated investigation of the individual processes. Any additional processes affecting observed stable isotope fractionation are considered as problematic for a CSIA-based assessment of contaminant fate (Druhan et al., 2019; Halloran et al., 2021; Rolle et al., 2010; Thullner et al., 2012), and our results thus indicate that phase-transition processes might be more relevant than considered so far and that they might generate a bias in the interpretation of CSIA data opposite to most of the phase-transition fractionation effects discussed in the literature to date.

CONCLUSIONS

The presented results suggest that the possibility of additional processes affecting stable isotope fractionation may need to be considered when interpreting stable isotope fractionation results for VOCs in systems containing a gas and a liquid phase. Given the widespread occurrence of such systems in the environment (e.g., all partially water-saturated subsurface compartments of the Critical Zone) a large number of environmental stable isotope analyses might be affected by such additional processes. We used a numerical approach to determine for two hypothesis (i.e. a very strong fractionation by the phase exchange, or degrading microorganisms located at the air-water interface taking up volatile substrate directly from the gas phase) their ability to explain the observed fractionation effects, but a detailed verification of these hypotheses was beyond the scope of our study and requires further investigations. Further research is thus needed to test the hypotheses discussed in this study or further hypotheses for explaining the presented observations and to eventually identify the processes responsible for the effects reported in this study.

SUPPLEMENTARY MATERIAL

Experimental results for Laper series A and B, and additional results of fitting the Laper results by the numerical simulations.

ACKNOWLEDGMENTS

This research was supported by the funding from Helmholtz Centre for Environmental Research – UFZ in the scope of the SAFIRA II Research Programme: Revitalization of Contaminated Land and Groundwater at Megasites, project Compartment Transfer II. The authors thank Dr. Asif Ali, Dr. Mohsin Kamal, and Dr. Sajid Ali for their assistance during this work.

REFERENCES

Aeppli, C., Berg, M., Cirpka, O.A., Holliger, C., Schwarzenbach, R.P. and Hofstetter, T.B. 2009. Influence of Mass-Transfer Limitations on Carbon Isotope Fractionation during Microbial Dechlorination of Trichloroethene. Environmental Science & Technology 43(23), 8813-8820.

Baertschi, P. and Kuhn, W. 1957. Dampfdruckunterschiede isotoper Verbindungen. (Infrarot-Anteil der Dispersionswechselwirkung als Ursache für grössere Flüchtigkeit der schweren Molekelspezies). Helvetica Chimica Acta 40(4), 1084-1103.

Bigeleisen, J. 1961. Statistical Mechanics of Isotope Effects on the Thermodynamic Properties of Condensed Systems. The Journal of Chemical Physics 34(5), 1485-1493.

Blum, P., Hunkeler, D., Weede, M., Beyer, C., Grathwohl, P. and Morasch, B. 2009. Quantification of biodegradation for o-xylene and naphthalene using first order decay models, Michaelis-Menten kinetics and stable carbon isotopes. Journal of Contaminant Hydrology 105(3-4), 118-130.

Bouchard, D., Höhener, P. and Hunkeler, D. 2008. Carbon Isotope Fractionation During Volatilization of Petroleum Hydrocarbons and Diffusion Across a Porous Medium: A Column Experiment. Environmental Science & Technology 42(21), 7801-7806.

Bouchard, D., Marchesi, M., Madsen, E.L., DeRito, C., Thomson, N.R., Aravena, R., Barker, J.F., Buscheck, T., Kolhatkar, R., Daniels, E.J. and Hunkeler, D. 2018. Diagnostic Tools to Assess Mass Removal Processes During Pulsed Air Sparging of a Petroleum Hydrocarbon Source Zone. Ground Water Monitoring and Remediation 38(4), 29-44.

Druhan, J.L., Winnick, M.J. and Thullner, M. 2019. Stable isotope fractionation by transport and transformation: When mass matters. Reviews in Mineralogiy and Geochemistry 85, 239-264.

Ehrl, B.N., Gharasoo, M. and Elsner, M. 2018. Isotope Fractionation Pinpoints Membrane Permeability as a Barrier to Atrazine Biodegradation in Gram-negative Polaromonas sp. Nea-C. Environ Sci Technol 52(7), 4137-4144.

406 Ehrl, B.N., Kundu, K., Gharasoo, M., Marozava, S. and Elsner, M. 2019. Rate-Limiting
407 Mass Transfer in Micropollutant Degradation Revealed by Isotope Fractionation in
408 Chemostat. Environ Sci Technol 53(3), 1197-1205.

409 Elsner, M. 2010. Stable isotope fractionation to investigate natural transformation
410 mechanisms of organic contaminants: principles, prospects and limitations. J.
411 Environ. Monit. 12(11), 2005-2031.

412 Elsner, M., Jochmann, M.A., Hofstetter, T.B., Hunkeler, D., Bernstein, A., Schmidt, T.C.
413 and Schimmelmann, A. 2012. Current challenges in compound-specific stable
414 isotope analysis of environmental organic contaminants. Anal. Bioanal. Chem. 403(9),
415 2471-2491.

416 Fischer, A., Bauer, J., Meckenstock, R.U., Stichler, W., Griebler, C., Maloszewski, P.,
417 Kästner, M. and Richnow, H.H. 2006. A multitracer test proving the reliability of
418 Rayleigh equation-based approach for assessing biodegradation in a BTEX
419 contaminated aquifer. Environmental Science & Technology 40(13), 4245-4252.

420 Gharasoo, M., Ehrl, B.N., Cirpka, O.A. and Elsner, M. 2019. Modeling of Contaminant
421 Biodegradation and Compound-Specific Isotope Fractionation in Chemostats at Low
422 Dilution Rates. Environ Sci Technol 53(3), 1186-1196.

423 Gharasoo, M., Thullner, M. and Elsner, M. 2017. Introduction of a new platform for
424 parameter estimation of kinetically complex environmental systems. Environ Model
425 Softw 98, 12-20.

426 Halloran, L.J.S., Vakili, F., Wanner, P., Shouakar-Stash, O. and Hunkeler, D. 2021.
427 Sorption- and diffusion-induced isotopic fractionation in chloroethenes. The Science
428 of the total environment 788, 147826.

429 Hanzel, J., Harms, H. and Wick, L.Y. 2010. Bacterial Chemotaxis along Vapor-Phase
430 Gradients of Naphthalene. Environmental Science & Technology 44(24), 9304-9310.

431 Hanzel, J., Thullner, M., Harms, H. and Wick, L.Y. 2011. Microbial growth with vapor-
432 phase substrate. Environmental Pollution 159(4), 858-864.

433 Horst, A. and Lacrampe-Couloume, G. 2020. Isotope fractionation ((2)H/(1)H,
434 (13)C/(12)C, (37)Cl/(35)Cl) in trichloromethane and trichloroethene caused by
435 partitioning between gas phase and water. Environmental science. Processes &
436 impacts 22(3), 617-626.

437 Horst, A., Lacrampe-Couloume, G. and Sherwood Lollar, B. 2016. Vapor Pressure
438 Isotope Effects in Halogenated Organic Compounds and Alcohols Dissolved in Water.
439 Anal Chem 88(24), 12066-12071.

440 Hunkeler, D. 2002. Quantification of isotope fractionation in experiments with
441 deuterium-labeled substrate. Applied and Environmental Microbiology 68(10), 5205-
442 5206.

443 Hunkeler, D. and Aravena, R. 2000. Determination of compound-specific carbon isotope
444 ratios of chlorinated methanes, ethanes, and ethenes in aqueous samples.
445 Environmental Science & Technology 34(13), 2839-2844.

446 Jeannottat, S. and Hunkeler, D. 2012. Chlorine and carbon isotopes fractionation during
447 volatilization and diffusive transport of trichloroethene in the unsaturated zone.
448 Environmental Science & Technology 46(6), 3169-3176.

449 Jeannottat, S. and Hunkeler, D. 2013. Can Soil Gas VOCs be Related to Groundwater
450 Plumes Based on Their Isotope Signature? Environ. Sci. Technol. 47(21), 12115-
451 12122.

452 Julien, M., Höhener, P., Robins, R.J., Parinnet, J. and Remaud, G.S. 2017. Position-
453 Specific ^{13}C Fractionation during Liquid–Vapor Transition Correlated to the Strength
454 of Intermolecular Interaction in the Liquid Phase. Journal of Physical Chemistry B
455 121(23), 5810-5817.

456 Kampara, M., Thullner, M., Harms, H. and Wick, L.Y. 2009. Impact of cell density on
457 microbially induced stable isotope fractionation. Applied Microbiology and
458 Biotechnology 81(5), 977-985.

459 Kampara, M., Thullner, M., Richnow, H.H., Harms, H. and Wick, L.Y. 2008. Impact of
460 bioavailability restrictions on microbially induced stable isotope fractionation. 2.
461 Experimental evidence. Environmental Science & Technology 42(17), 6552-6558.

462 Khan, A.M., Wick, L.Y., Harms, H. and Thullner, M. 2016. Biodegradation of vapor-phase
463 toluene in unsaturated porous media: Column experiments. Environ. Pollut. 211, 325-
464 331.

465 Khan, A.M., Wick, L.Y. and Thullner, M. 2018. Applying the Rayleigh Approach for Stable
466 Isotope-Based Analysis of VOC Biodegradation in Diffusion-Dominated Systems.
467 Environ Sci Technol 52(14), 7785-7795.

468 Kopinke, F.D., Georgi, A. and Roland, U. 2018. Isotope fractionation in phase-transfer
469 processes under thermodynamic and kinetic control - Implications for diffusive
470 fractionation in aqueous solution. The Science of the total environment 610-611, 495-
471 502.

472 Kuder, T., Philp, P. and Allen, J. 2009. Effects of Volatilization on Carbon and Hydrogen
473 Isotope Ratios of MTBE. Environmental Science & Technology 43(6), 1763-1768.

474 Marozava, S., Meyer, A.H., Perez-de-Mora, A., Gharasoo, M., Zhuo, L., Wang, H., Cirpka,
475 O.A., Meckenstock, R.U. and Elsner, M. 2019. Mass Transfer Limitation during Slow
476 Anaerobic Biodegradation of 2-Methylnaphthalene. Environ Sci Technol 53(16),
477 9481-9490.

478 Morasch, B., Richnow, H.H., Schink, B. and Meckenstock, R.U. 2001. Stable hydrogen
479 and carbon isotope fractionation during microbial toluene degradation: Mechanistic

480 and environmental aspects. Applied and Environmental Microbiology 67(10), 4842-
481 4849.

482 Nancharaiah, Y.V., Wattiau, P., Wuerz, S., Bathe, S., Mohan, S.V., Wilderer, P.A. and
483 Hausner, M. 2003. Dual labeling of Pseudomonas putida with fluorescent proteins
484 for in situ monitoring of conjugal transfer of the TOL plasmid. Applied and
485 Environmental Microbiology 69, 4846-4852.

486 Rolle, M., Chiogna, G., Bauer, R., Griebler, C. and Grathwohl, P. 2010. Isotopic
487 Fractionation by Transverse Dispersion: Flow-through Microcosms and Reactive
488 Transport Modeling Study. Environmental Science & Technology 44(16), 6167-6173.

489 Rolle, M. and Jin, B. 2017. Normal and Inverse Diffusive Isotope Fractionation of
490 Deuterated Toluene and Benzene in Aqueous Systems. Environmental Science &
491 Technology Letters 4(7), 298-304.

492 Ross, S.M. (2017) Introductory Statistics, Academic Press.

493 Rostkowski, M., Schurner, H.K.V., Sowinska, A., Vasquez, L., Przydacz, M., Elsner, M. and
494 Dybala-Defratyka, A. 2021. Isotope Effects on the Vaporization of Organic
495 Compounds from an Aqueous Solution-Insight from Experiment and Computations. J
496 Phys Chem B 125(51), 13868-13885.

497 Sander, R. 2015. Compilation of Henry's law constants (version 4.0) for water as solvent.
498 Atmospheric Chemistry and Physics 15(8), 4399-4981.

499 Schwarzenbach, R.P., Gschwend, P.M. and Imboden, D.M. (2003) Environmental Organic
500 Chemistry 2nd ed., Wiley, New York.

501 Scott, K.M., Lu, X., Cavanaugh, C.M. and Liu, J.S. 2004. Optimal methods for estimating
502 kinetic isotope effects from different forms of the Rayleigh distillation equation.
503 Geochimica Et Cosmochimica Acta 68(3), 433-442.

504 Slater, G.F., Dempster, H.S., Sherwood, L.B. and Ahad, J. 1999. Headspace Analysis: A
505 New Application for Isotopic Characterization of Dissolved Organic Contaminants.
506 Environ. Sci. Technol. 33(1), 190-194.

507 Sun, F., Mellage, A., Gharasoo, M., Melsbach, A., Cao, X., Zimmermann, R., Griebler, C.,
508 Thullner, M., Cirpka, O.A. and Elsner, M. 2021a. Mass-Transfer-Limited
509 Biodegradation at Low Concentrations-Evidence from Reactive Transport Modeling
510 of Isotope Profiles in a Bench-Scale Aquifer. Environ Sci Technol 55(11), 7386-7397.

511 Sun, F., Peters, J., Thullner, M., Cirpka, O.A. and Elsner, M. 2021b. Magnitude of
512 Diffusion- and Transverse Dispersion-Induced Isotope Fractionation of Organic
513 Compounds in Aqueous Systems. Environ Sci Technol 55, 4772-4782.

514 Thullner, M., Centler, F., Richnow, H.-H. and Fischer, A. 2012. Quantification of organic
515 pollutant degradation in contaminated aquifers using compound specific stable
516 isotope analysis – Review of recent developments. Org. Geochem. 42(12), 1440-1460.

517 Thullner, M., Fischer, A., Richnow, H.H. and Wick, L.Y. 2013. Influence of mass transfer
518 on stable isotope fractionation. Applied Microbiology and Biotechnology 97(2), 441-
519 452.

520 Thullner, M., Kampara, M., Richnow, H.H., Harms, H. and Wick, L.Y. 2008. Impact of
521 bioavailability restrictions on microbially induced stable isotope fractionation. 1.
522 Theoretical calculation. Environmental Science & Technology 42(17), 6544-6551.

523 Wiedemeier, T.H., Rifai, H.S., Newell, C.J. and Wilson, J.T. 1999. Natural Attenuation of
524 Fuels and Chlorinated Solvents in the Subsurface. John Wiley, New York.

525 Wolfsberg, M. 1963. Isotope effects on intermolecular interactions and isotopic vapor
526 pressure differences. J. Chim. Phys. 60, 15-22.
527

528 **FIGURES AND TABLES**

529

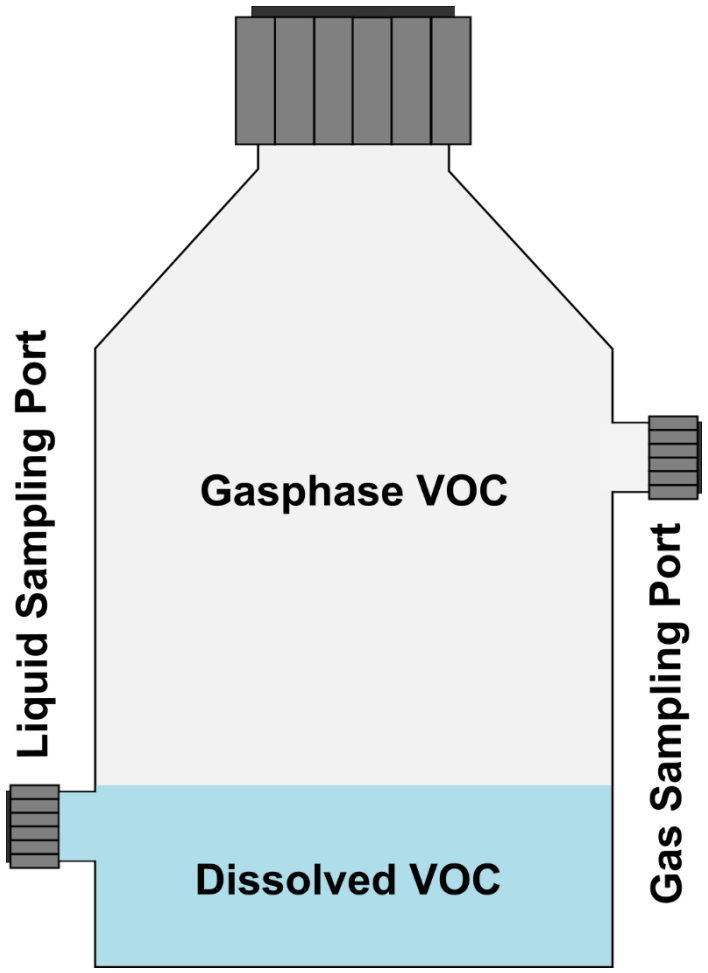

530
531

532 **Figure 1:** Sketch of a liquid-air phase exchange reactors (Laper). Gastight chromoflax
533 glass bottles with total volume of 1150 mL (series A) and 2375 mL (series B), filled with
534 200 mL (series A) and 400 mL (series B) minimal media (amended with the VOCs
535 (toluene and MTBE) and toluene degrading bacteria) leaving 950 mL (series A) and 1875
536 mL (series B) headspace.

537

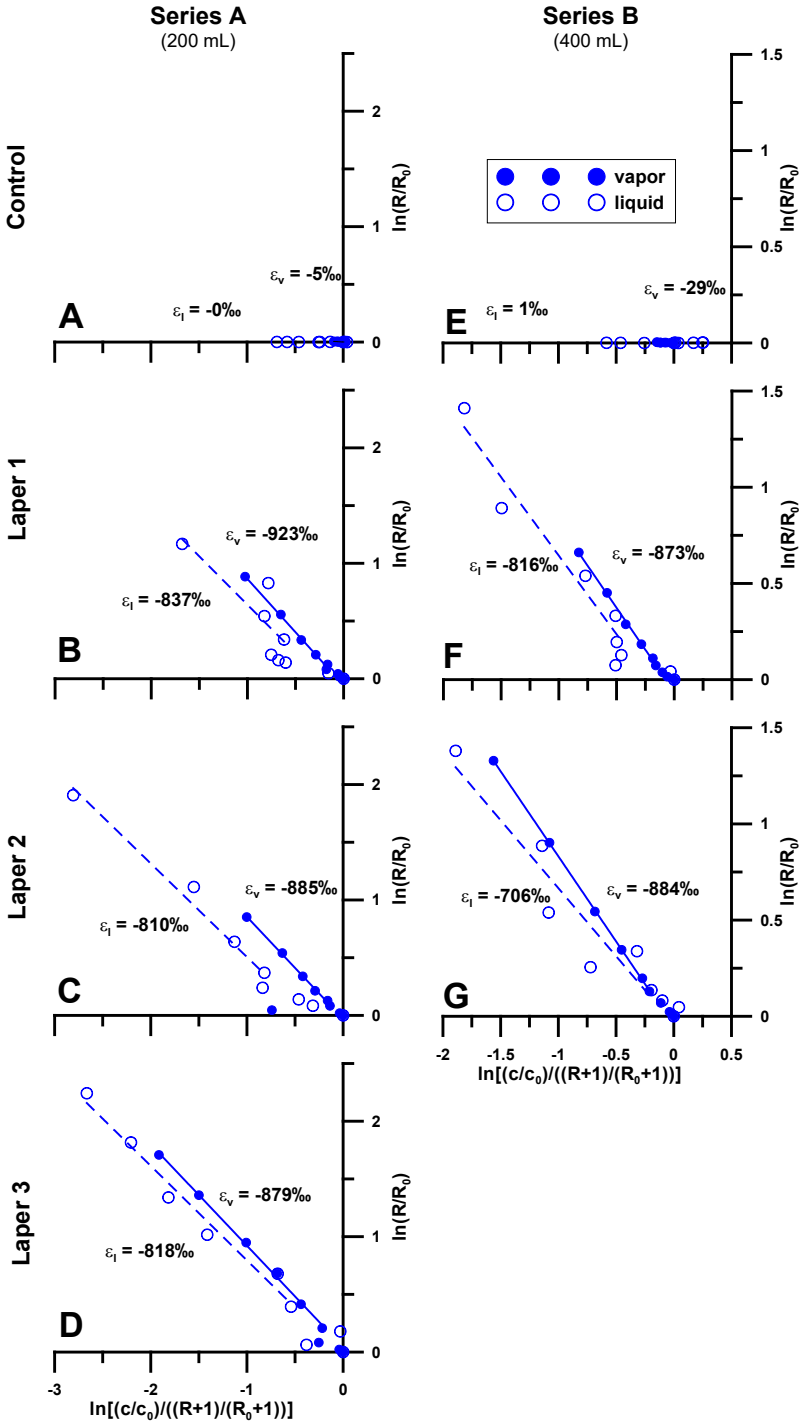

538

539 **Figure 2:** Rayleigh plots showing measured stable isotope fractionation in the gas and
540 liquid phase of Laper series A (200 mL; left column, panels A to D) and B (400 mL; right
541 columns, panels E to G). To avoid possible effects from initial disturbances, shown linear
542 fits considered only data from 3 to 8 hours. The first row (panels A and E) represents
543 abiotic control, second row (panels B and E) shows Laper 1 and third row (panels C and
544 G) Laper 2, the last row (panel D) shows Laper 3.

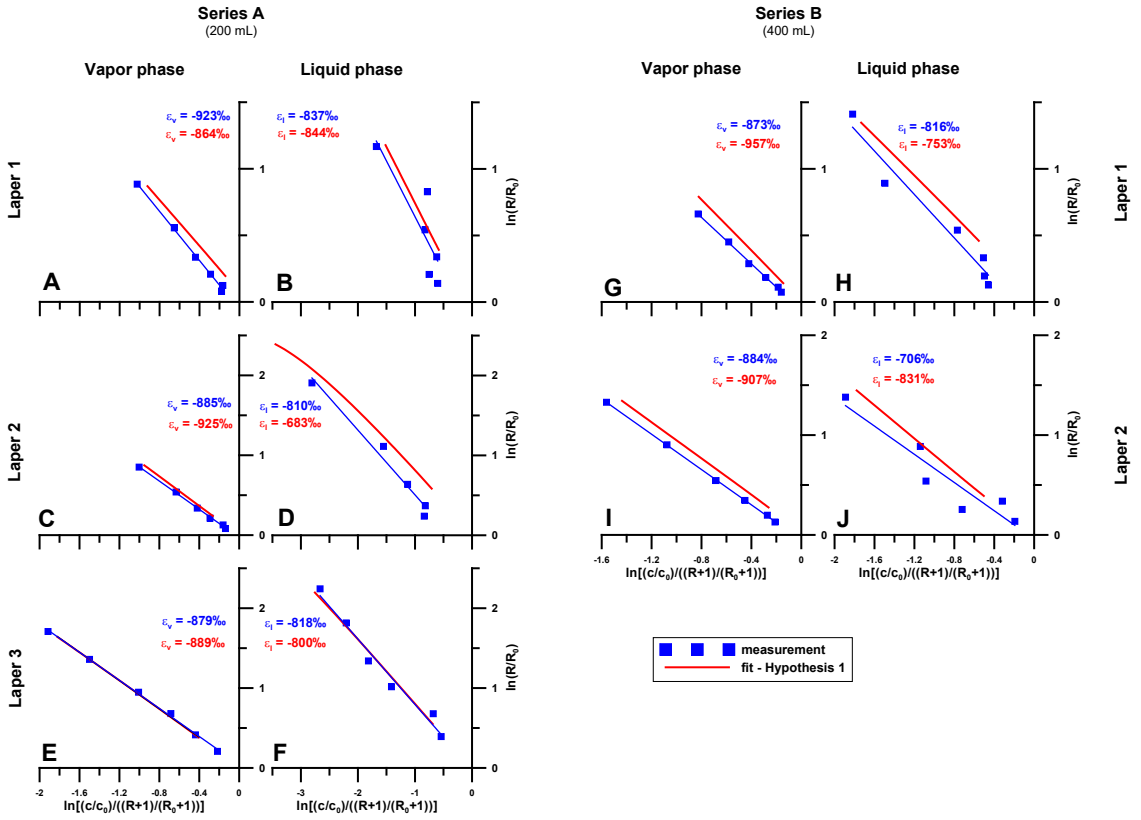

Figure 3: *Hypothesis 1*: Rayleigh plots showing comparison of measured and fitted data for Laper series A (panels A to F) and Laper series B (panels G to H). Blue symbols represent experimental data, blue lines are linear regression of measured data, and red solid lines are fitted values allowing for a high fractionation due to the phase exchange. Rayleigh plots show only results for the observation time between 3 and 8 hours.

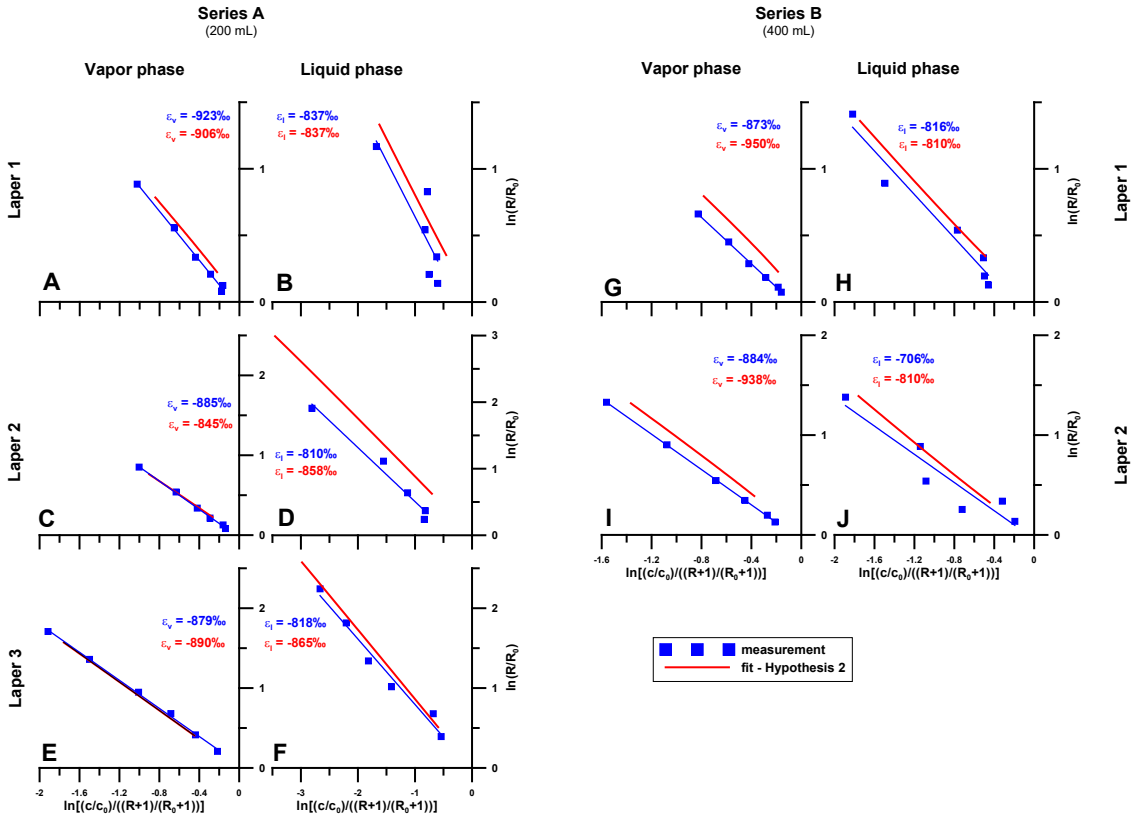

551

552 **Figure 4**: *Hypothesis 2*: Rayleigh plots showing comparison of measured and fitted data
553 for Laper series A (panels A to F) and Laper series B (panels G to H). Blue symbols
554 represent experimental data, blue lines are linear regression of measured data, and red
555 solid lines are fitted values (for series A with constrained phase exchange rate parameter).
556 Rayleigh plots show only results for the observation time between 3 and 8 hours.

557

Table1: *Hypothesis 1*: Parameter values obtained by fitting. Value constraints are [1] assumed, [2] taken form Sander (2015), [3] taken from Khan et al. (2018). Errors for the measured enrichment factors are standard deviations determined from the slopes of the Rayleigh plots.

				Series A (200 mL)			Series B (400 mL)		
			unit	**Laper 1**	**Laper 2**	**Laper 3**	**Laper 1**	**Laper 2**	**Constraints**
Fitted parameters		k_{max}	mg L^{-1} h^{-1}	4.98	5.06	6.68	5.66	4.39	
		K_s	mg L^{-1}	0.1	0.122	0.813	0.1	0.1	0.1-10 [1]
		k_{ex}	h^{-1}	3.92	0.814	3.08	1.61	12.9	
		$^{l}H, ^{h}H$	-	0.35	0.225	0.35	0.23	0.2	0.2-0.35 [2]
		ε_b	‰	-870	-870	-886	-870	-870	-(870-970) [3]
		ε_{ex}	‰	-454	-900	-727	-900	-900	-(0-900) [1]
Fitting results		ε_v	‰	-864	-925	-889	-957	-907	
		ε_l	‰	-844	-683	-800	-753	-831	
Mea-sured results		ε_v	‰	-923 ± 28	-885 ± 18	-879 ± 19	-873 ± 19	-884 ± 6	
		ε_l	‰	-837 ± 261	-810 ± 77	-818 ± 65	-816 ± 90	-706 ± 128	

565 **Table2**: *Hypothesis 2*: Parameter values obtained by fitting. Value constraints are [1)]
566 taken from Khan et al. (2018), [2)] values for series A systems constrained to approx.
567 value range fitted for series B systems [3)] taken from Sander (2015), [4)] taken from Sun et
568 al. (2021b). Errors for the measured enrichment factors are standard deviations
569 determined from the slopes of the Rayleigh plots.

570

			Series A (200 mL)			Series B (400 mL)		
		unit	Laper 1	Laper 2	Laper 3	Laper 1	Laper 2	Constraints
Fitted parameters	k_{max}	mg L^{-1} h^{-1}	2.66	2.98	2.89	3.07	2.17	
	$k_{max,g}$	mg L^{-1} h^{-1}	0.626	0.568	0.912	0.645	0.731	
	K_s	mg L^{-1}	0.5	0.5	0.5	0.5	0.5	0.5 [1)]
	k_{ex}	h^{-1}	0.3	0.1	0.3	0.321	0.166	0.1-0.3 [2)]
	^{l}H, ^{h}H	-	0.35	0.35	0.35	0.35	0.35	0.2-0.35 [3)]
	ε_b	‰	-870	-870	-870	-870	-870	-(870-970) [1)]
	$\varepsilon_{b,g}$	‰	-870	-870	-898	-870	-870	-(870-970) [1)]
	ε_{ex}	‰	0	-50	-50	0	-50	-(0-50) [4)]
Fitting results	ε_v	‰	-906	-845	-891	-950	-938	
	ε_l	‰	-837	-858	-865	-810	-810	
Mea-sured results	ε_v	‰	-923 ± 28	-885 ± 18	-879 ± 19	-873 ± 19	-884 ± 6	
	ε_l	‰	-837 ± 261	-810 ± 77	-818 ± 65	-816 ± 90	-706 ± 128	

571

572